QoE Enhancement by Capacity Allocation and Piggyback Bandwidth Request in Audio–Video IP Transmission over the IEEE 802.16 BE Service

Toshiro Nunome and Shuji Tasaka
Department of Computer Science and Engineering, Graduate School of Engineering,
Nagoya Institute of Technology, Nagoya 466–8555, Japan
Email: {nunome, tasaka}@nitech.ac.jp

***Abstract*—This paper studies QoE (Quality of Experience) enhancement of audio–video IP transmission over the uplink channel, i.e., from subscriber stations (SSs) to the base station (BS), in the IEEE 802.16 BE service. We assume two types of capacity allocation schemes for uplink and downlink burst durations: static and adaptive. Furthermore, we introduce a piggyback request mechanism for uplink bandwidth requests from SSs to the BS in addition to a random access–based request mechanism. We assess QoE of audio–video streams for four schemes obtained from the combination of the bandwidth request mechanisms and the capacity allocation schemes. We also employ two types of audio–video contents. From the assessment result, we notice that the piggyback request mechanism can enhance QoE of audio–video transmission. In addition, the adaptive allocation scheme is effective for QoE enhancement particularly under heavily loaded conditions because of its efficient usage of OFDM symbols. We also find that the effects of piggyback request mechanism and capacity allocation schemes on QoE change according to the content types.**

***Keywords*-IEEE 802.16, WiMAX, Audio–Video streaming, QoE, QoS**

I. Introduction

The ultimate goal of the network services is to provide high *QoE (Quality of Experience)* [1], which is perceptual quality for users. It is desirable to design and operate the network systems in order to maximize the QoE.

Rich multimedia services with high quality audio and video streaming bring great demands for *Broadband Wireless Access (BWA)* to the Internet for residential users. Not only downlink capacity but also uplink capacity is required owing to personal streaming services such as Ustream [2].

The *WirelessMAN–OFDM TDD* is a profile specified in IEEE 802.16–2004 [3]; it is also known as *Fixed WiMAX (Worldwide Interoperability for Microwave Access)* [4], for fixed BWA systems. In the system, the uplink to downlink bandwidth ratio can vary with time to optimize network performance.

Chiang *et al*. examine the impact of improper bandwidth ratio between uplink and downlink channels on the performance of TCP and propose an Adaptive Bandwidth Allocation Scheme (ABAS) which adjusts the bandwidth ratio according to the current traffic profile [5]. The scheme is specified only for TCP and therefore not appropriate for other transport protocols. They assess the effectiveness only at the transport layer.

Pries *et al*. discuss an adaptive subframing in the WirelessMAN–OFDM TDD system [6]. They propose an algorithm for a dynamic setting of the uplink and downlink ratio. The performance of the proposed algorithm is evaluated in VoIP, Web, and FTP traffic. They do not consider audio–video transmission.

Because the current Internet mainly provides *Best Effort (BE)* services, many applications and services are brought with the BE service while the IEEE 802.16 has a framework for QoS provisioning.

The *broadcast polling* is the default operation for uplink channel access in the BE service. The bandwidth request messages are sent during the contention period in the uplink subframe, and the bandwidth is assigned only when the messages have been accepted.

As the size of the contention period increases, collisions among requests occur less frequently; it improves uplink performance. However, the increase of contention period leads to decline of the capacity for uplink and downlink data transmission. That is, there exists a tradeoff between the capacity and the request efficiency.

In the BE service, subscriber stations (SSs) are also allowed to ask for bandwidth via piggyback request with the broadcast polling. The piggyback request mechanism can reduce the collisions in the contention period and then improves efficiency of bandwidth request.

A variety of studies on audio–video transmission in IEEE 802.16 networks have been reported. However, there are few studies which consider QoE. We cannot find any report on QoE–based discussion about the tradeoff between the capacity and the request efficiency for audio–video transmission over IEEE 802.16/WiMAX networks.

In [7], Migliorini *et al*. propose a simulation framework to assess QoE of video streaming over WiMAX networks. Nevertheless, they assume only *PSNR (Peak Signal to Noise Ratio)*, which measures spatial quality of video at the *application–level*, for the quality metric. They also consider video only; that is, no audio.

Lee and Song have presented a QoE–aware channel control algorithm for mobile IPTV services over WiMAX networks [8]. They deal with the channel zapping time as a QoE metric and discuss an effective tradeoff between the channel zapping time and the video quality. However, they assess the video quality by PSNR and do not perform systematic QoE assessment of audio–video streams.

In this paper, we treat QoE as users' perceptual quality and enhance QoE of audio–video IP transmission over the IEEE 802.16 network by means of capacity allocation and the piggyback request mechanism. We assume a WirelessMAN–OFDM TDD network with the BE service. We employ two strategies of capacity allocation: adaptive and static. The *adaptive allocation scheme* dynamically allocates the capacity between uplink and downlink according to request. The *static allocation scheme* statically allocates the capacity to each direction. We introduce the piggyback request mechanism for uplink bandwidth requests from SSs to the base station (BS) in addition to the random access–based request mechanism, i.e., the broadcast polling. By a subjective experiment, we assess QoE of audio–video streams for four schemes obtained from the combination of the bandwidth request mechanisms and the capacity allocation schemes.

The rest of this paper is organized as follows. Section II summarizes the IEEE 802.16 WirelessMAN–OFDM specification. Section III illustrates a methodology for the simulation, including the network configuration, simulation method, and QoS parameters. The experimental method of QoE assessment is explained in Section IV. The QoE/QoS assessment results

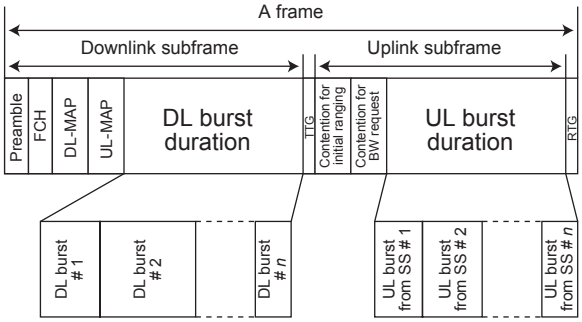

Fig. 1. MAC frame structure.

are presented and discussed in Section V. Finally, Section VI concludes this paper.

II. IEEE 802.16

The IEEE 802.16–2004 specifies several profiles for the physical and MAC layers. In this paper, we treat the WirelessMAN–OFDM TDD system.

A. Frame Structure

The structure of a frame is shown in Fig. 1. The frame is divided into two subframes: *downlink (DL)* and *uplink (UL)* subframes. The uplink subframe follows the downlink one. The resource is allocated in each subframe in units of OFDM symbol. *TTG (transmit/receive transition gap)* and *RTG (receive/ transmit transition gap)* are inserted between the subframes to allow the station to switch between transmission and reception operation modes.

The downlink subframe includes *DL–MAP (downlink map)* and *UL–MAP (uplink map)*, which include allocation information of the burst duration for downlink and uplink subframes, respectively.

The uplink subframe includes two contention periods; one is for initial ranging, and the other is for bandwidth request. Each contention period consists of a number of slots for contention–based access. BS announces these periods by means of UL–MAP in the preceding downlink subframe.

In the downlink subframe, BS transmits a burst of MAC protocol data units (PDUs). On the other hand, in the uplink subframe, an SS to which the bandwidth is assigned through UL–MAP transmits a burst of MAC PDUs to BS in a time–division multiple access (TDMA) manner.

In this paper, we focus on the BE scheduling service, in which an SS asks for bandwidth for a connection by sending a request to BS within the bandwidth request contention slots in the uplink subframe; that is, the broadcast polling is employed.

B. Capacity Allocation Scheme

In this section, we explain capacity allocation schemes for the BE service employed in this paper.

The static allocation scheme statically splits the bandwidth between uplink and downlink burst durations. The required bandwidth for each burst duration changes according to channel condition and applications, and then the static allocation may lead to inefficient bandwidth utilization.

The adaptive allocation scheme dynamically allocates OFDM symbols to uplink and downlink burst durations. If there is enough capacity to accept the whole requested bandwidth, BS assigns the bandwidth as requested. Otherwise, BS proportionally assigns the bandwidth for uplink and downlink burst durations. In each duration, the bandwidth is assigned to each service flow on a round–robin basis.

Here, we describe the procedure of capacity allocation in the adaptive allocation scheme. Let B denote OFDM symbols available for DL and UL burst durations. We divide them into B_d symbols for downlink and B_u symbols for uplink. We also assume that n SSs are connected to BS. BS collects information of the requested bandwidth from each SS; $r_{d,i}$ $(i = 1, 2, \cdots, n)$ represents the required bandwidth for downlink from BS to SSi in bytes, while $r_{u,i}$ the requested bandwidth for uplink from SSi. Furthermore, let $R_{d,i}$ and $R_{u,i}$ be the number of OFDM symbols necessary to transmit $r_{d,i}$ bytes data and that for $r_{u,i}$ bytes data, respectively. Note that the number of bytes which can be transmitted by an OFDM symbol depends on modulation and coding schemes in the physical layer.

Next, BS calculates the requested bandwidth in symbols for the whole downlink connections TR_d and that for the whole uplink connections TR_u as

$$TR_d = \sum_{i=1}^{n} R_{d,i} \quad (1)$$

$$TR_u = \sum_{i=1}^{n} R_{u,i} \quad (2)$$

Then, BS divides B OFDM symbols as follows.

if $(TR_d + TR_u) \leq B$ **then**
  $B_u \leftarrow TR_u$
  $B_d \leftarrow TR_d$
else
  $B_u \leftarrow round\left(\frac{TR_u}{TR_d+TR_u} \times B\right)$
  $B_d \leftarrow B - B_u$
end if

Here, the $round(x)$ function rounds x to the nearest integer.

Bandwidth demands for downlink connections, i.e., $r_{d,i}$, are estimated on the basis of the queue length of each connection in bytes. A queue of packets at the network layer is formed in each connection, and the maximum length of each connection queue is set to 50 in this paper.

For uplink, in the same way, each SS requests the bandwidth, i.e., $r_{u,i}$, via the broadcast polling mechanism. BS grants the SS at most one transmission opportunity in each uplink subframe, and the SS can transmit data frames within the granted transmission opportunity.

In the broadcast polling mechanism, an SS contends for the bandwidth request contention slots to send a request message to BS. When the request message collides, the SS retries the transmission after an exponential backoff. The number of contention slots in each frame is one of the important system parameters which affect the performance.

In this paper, we change the number of contention slots in each frame to find the number which maximizes QoE of audio–video IP transmission.

C. Piggyback Request Mechanism

Each SS can piggyback the bandwidth request to a MAC PDU to be transmitted when the SS has data to transmit and needs to request additional bandwidth. For the bandwidth request to BS, the SS uses the Grant Management Subheader, whose length is two bytes, of the first MAC PDU in the burst of PDUs.

III. Simulation

In this paper, we performed computer simulation with ns–2 [9]; we have employed a simulation model developed by NIST [10] and modified by TELECOM Bretagne [11] for the assessment.

A. Network Configuration

Figure 2 illustrates the network configuration in the simulation. SSk $(k = 1, 2, \cdots, n)$ denotes a wireless node, which is located on a circle of 100 m radius from BS. LNk is a wired node, which is connected to BS via router R. Each

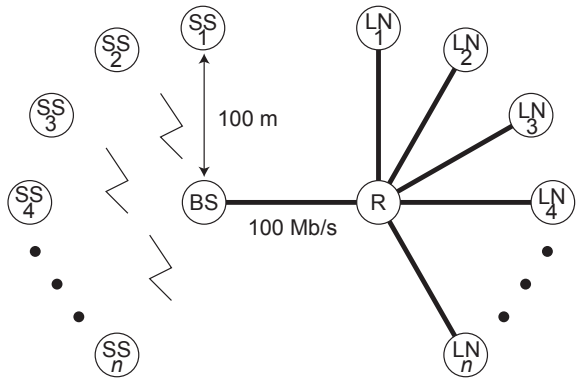

Fig. 2. Network configuration.

TABLE I
PHYSICAL LAYER PARAMETERS IN SIMULATION.

parameter	value
FFT size	256
frequency	3.486 GHz
channel bandwidth	7 MHz
frame size	5 ms
guard interval	2 μs
physical slot length	500 ns
modulation	64QAM 3/4
symbol time	34 μs
number of bits per symbol	856 bits/symbol

wired connection is a 100 Mb/s duplex link in which the propagation delay between BS and LNk is 1 ms. Among the pairs of wireless and wired nodes, we employ the pair of SS1 and LN1 as the audio–video nodes for uplink. The pair of SS2 and LN2 is also the audio–video nodes for downlink, and we use the other nodes as the background traffic nodes.

Table I shows the physical layer parameters in the simulation. These parameter values have been selected in accordance with the certification profile of Fixed WiMAX [4]. These parameters are also supported in the current IEEE 802.16 compliant devices such as [12] and [13]. From the parameters, we can calculate the maximum transmission speed in the physical layer as about 25.23 Mb/s. We employ the TwoRayGround model as the wireless propagation model and assume random errors; its bit error rate is 1.0×10^{-7}.

The size of a contention slot for the bandwidth request is two OFDM symbols. A preamble consumes one symbol, and the other symbol is enough to transmit the bandwidth request.

B. Method of Simulation

SS1 and LN2 are the audio and video sources, and LN1 and SS2 are the receivers; one node transmits the media streams to the other node with RTP/UDP. We use two types of audio–video stream for uplink transmission, i.e., from SS1 to LN1. The contents are sport and music video as shown in Table II. From LN2 to SS2, we transmit the audio–video stream of a scene of movie, in which a man rides a bicycle.

Table III shows the specifications of the audio and video for uplink transmission. We refer to the transmission unit at the application–level as the *Media Unit (MU)*; a video frame is defined as a video MU, and a constant number of audio samples as an audio MU. As for the audio–video stream transmitted from LN2, the average bit rate of audio and that for video are 192 kb/s and 810.48 kb/s, respectively; the average MU rate of audio is 25 MU/s, and that of video is 20 MU/s.

In the audio–video transmission with the BE service, receiver–buffering control is necessary for absorbing network

TABLE II
CONTENTS USED IN THE EXPERIMENT.

content	scenes
sport	A man is snowboarding. The view is captured from the sky. The scene is video dominant.
music video	Three men are playing music. The scene is audio dominant.

TABLE III
SPECIFICATIONS OF AUDIO AND VIDEO FOR UPLINK.

	audio	video
coding method	PCM 24 kHz 8bit 1ch	H.264 (JM 16.2) GOP IPPPP
picture size [pixels]	—	320 × 240
average MU size [bytes]	960	(sport) I: 10858, P: 3481 (music video) I: 7828, P: 4442
average MU rate [MU/s]	25.0	20.0
average MU interval [ms]	40.0	50.0
average bit rate [kb/s]	192.0	(sport) 793.48 (music video) 819.12
duration [sec]	120.0	

delay jitter. Thus, we adopt a simple playout buffering control scheme [14]. The buffering time is set to 200 ms[1].

As the error concealment technique in this paper, we employ the one implemented in H.264/MPEG–4 AVC reference software JM16.2. For I–frames, we utilize the spatial approach: A missing block is interpolated from its neighboring blocks in the current frame. For P–frames, two techniques of the temporal approach are available: Frame Copy and Motion Copy. The former simply replaces the missing block with the spatially corresponding one of the previously output frame, while the latter utilizes the information of the motion vector in the replacement. This paper selects the Frame Copy scheme for simplicity.

SSk' and LNk' ($k' = 3, 4, \cdots, n$) are used to handle background traffic flows for the audio and video streams. A pair of SSk' and LNk' is referred to as a *load terminal pair*. We suppose that the number of load terminal pairs is 18 ($n = 20$) or 20 ($n = 22$). SSk' sends/receives the traffic to/from LNk'. The nodes generate fixed–size IP datagrams of 1500 bytes each at exponentially distributed intervals. The amount of the traffic is adjusted by changing the average of the interval. We refer to the average amount of the traffic for each load terminal as the *average load*. In this study, we set the average load for each uplink load terminal, i.e., SSk', to 150 kb/s. In addition, the average load for each downlink load terminal, i.e., LNk', is set to 350 kb/s.

In this paper, we employ the adaptive allocation scheme or the static allocation scheme introduced in Subsection II-B. The adaptive allocation scheme assigns the bandwidth to uplink and downlink burst durations dynamically. The static allocation scheme splits the bandwidth between the uplink and downlink burst durations at a ratio of three to seven; it is an appropriate setting for the traffic condition considered in this paper. We also change the number of contention slots per frame from three through twelve slots. In addition, we consider two cases: with the piggyback mechanism and without the piggyback mechanism.

C. QoS Parameters

As application–level QoS parameters for video, we employ the *error concealment ratio* [15] and the *MU loss ratio*. The

[1]We will investigate the influence of the buffering time on QoE as future work.

error concealment ratio represents the percentage of slices error–concealed (i.e., lost slices) in a frame. The MU loss ratio is the ratio of the number of MUs not output at the recipient to the number of MUs transmitted by the sender.

On the other hand, we utilize the *number of received bandwidth requests* as the MAC–level QoS parameter. It shows the total number of bandwidth requests received by BS from each SS during audio–video transmission.

IV. Experiment for QoE Assessment

In this paper, we assess the QoE of the audio–video stream by a subjective experiment. It was conducted as follows.

We first made test samples for subjective assessment by actually outputting the audio and video MUs with the output timing obtained from the simulation. The test samples are called *stimuli*. Each stimulus lasts 15 seconds and was obtained by outputting the audio–video stream from time 105 to 120 in seconds after starting the transmission in the simulation.

We put the stimuli in a random order and presented them to 21 assessors. The assessors are male and female in their twenties or thirties. They are 20 Japanese students and a non–Japanese student who can understand the Japanese language.

A subjective score is measured by the *rating–scale method*, in which assessors classify each stimulus into one of a certain number of categories. We adopted the following five categories of *impairment*: "imperceptible" assigned integer 5, "perceptible, but not annoying" 4, "slightly annoying" 3, "annoying" 2, and "very annoying" 1. The integer value is regarded as the subjective score.

Note that almost all recommendations by ITU–T and ITU–R use the *mean opinion score (MOS)* as the objective measure of perceptual quality; the MOS value for a stimulus is calculated by averaging the scores measured by the rating–scale method over all assessors. However, in the strict sense, MOS is an *ordinal scale*, which only has a greater–than–less–than relation between scores given by the assessors. In the calculation of MOS, we implicitly assume that the difference between any two successive scores means the same magnitude of the assessor's sensation (e.g., "$5-4$" has the same meaning as "$3-2$" for all assessors). This can be approximately valid for assessment of a single medium, i.e., audio only or video only; however, cross–modal influences of multimedia can invalidate the assumption. It is desirable for us to use at least an *interval scale*, where the intervals between the scale values represent differences or distances between amounts of the sensory attribute measured.

In this paper, we utilize the *method of successive categories* [16] in order to obtain an interval scale as the QoE metric. We first measure the frequency of each category with which stimulus was placed in the category by the rating–scale method. With the *law of categorical judgment*, we can translate the frequency obtained by the rating–scale method into an interval scale. We then perform Mosteller's test, which tests the goodness of fit between the obtained interval scale and the measurement result. The interval scale for which we have confirmed the goodness of fit is referred to as the *psychological scale*.

V. Assessment Results

From the simulation results, we found that the application–level QoS of the audio–video stream transmitted over the downlink connection scarcely degrades under all the conditions considered here; the application–level QoS is closely related to the QoE. Therefore, we focus on the QoE and QoS of the uplink connection only.

In this section, we first show the assessment results of MAC–level and application–level QoS. We then discuss the QoE assessment results. In the MAC–level and application–level QoS assessment, there is little difference between the two contents. Thus, we present the results of QoS assessment for music video.

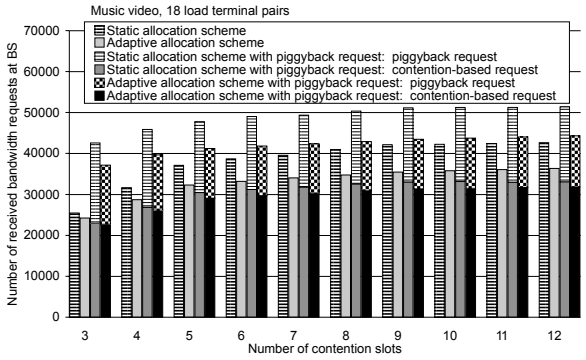

Fig. 3. Number of bandwidth requests for music video with 18 load terminal pairs.

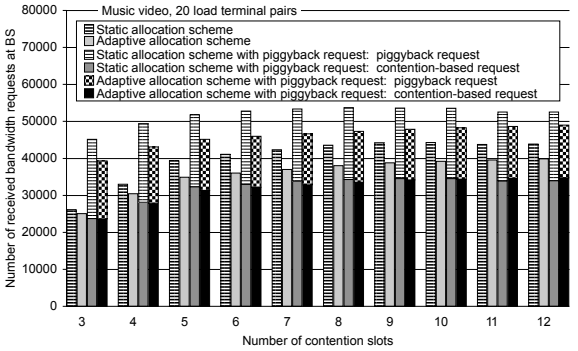

Fig. 4. Number of bandwidth requests for music video with 20 load terminal pairs.

A. MAC–Level QoS

Figure 3 depicts the number of bandwidth requests received by BS with 18 load terminal pairs versus the number of contention slots. The figure shows the results of four schemes obtained from the combination of the bandwidth request mechanisms and the capacity allocation schemes. In addition, for the schemes with the piggyback request, we distinguish the number of requests by the broadcast polling and that by the piggyback request. Figure 4 depicts the number of requests with 20 load terminal pairs.

We notice in Figs. 3 and 4 that the total number of received bandwidth requests with the piggyback bandwidth request mechanism is larger than that without the piggyback mechanism for all the number of contention slots considered here and both capacity allocation schemes. In addition, we also find that the number of received requests during the contention–based request phase in the scheme with the piggyback mechanism is smaller than that without the piggyback mechanism. Thus, owing to the piggyback mechanism, each SS can transmit the bandwidth requests efficiently.

In Figs. 3 and 4, we see that the number of received requests in all the schemes increases as the number of contention slots increases from three to eight. This is because the efficiency of the contention–based request improves as the number of contention slots increases.

On the other hand, in Fig. 3, when the number of contention slots is equal to or larger than nine, we notice that the number of received requests is not affected by the number of slots. Thus, in the situation assumed in Fig. 3, the sufficient number of contention slots is nine or larger.

We see in Fig. 4 that when the number of contention slots is eleven or twelve, the number of received request with the static allocation scheme is slightly smaller than that for ten contention slots. For 20 load terminal pairs with the static

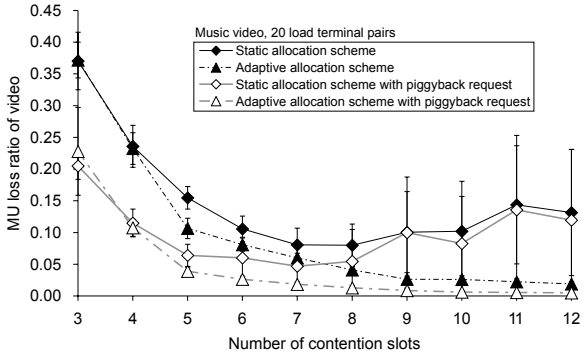

Fig. 5. MU loss ratio of video for music video with 20 load terminal pairs.

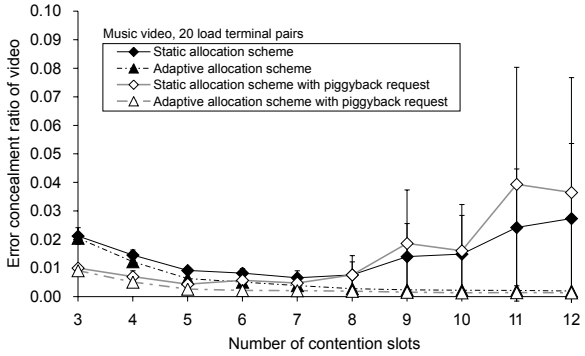

Fig. 6. Error concealment ratio of video for music video with 20 load terminal pairs.

allocation scheme, as the number of contention slots increases, the number of OFDM symbols for uplink burst duration decreases; it causes the shortage of uplink bandwidth. Under the condition, BS cannot allocate the bandwidth immediately after receiving the request. It causes the decrement of the number of bandwidth requests.

In Figs. 3 and 4, we see that the number of requests with the adaptive allocation scheme is smaller than that with the static allocation scheme whether the piggyback request is available or not. The reason is as follows. The static allocation scheme sometimes cannot assign the bandwidth as requested because the capacity is limited by the predetermined ratio. Thus, the static allocation scheme needs to request bandwidth more often because of partially granted bandwidth.

B. Application–Level QoS

Figures 5 and 6 depict the MU loss ratio of video and the error concealment ratio of video, respectively, as a function of the number of contention slots for 20 load terminal pairs. In these figures, we also show 95 % confidence intervals. However, when the interval is smaller than the size of the corresponding symbol representing the simulation result, we do not show it in the figures. We have also assessed the MU loss ratio of audio; it has the same tendency as that of video.

In Fig. 5, we find that in the static allocation scheme, the number of contention slots which minimizes the MU loss ratio of video exists. On the other hand, in the adaptive allocation scheme, for the number of contention slots considered here, the MU loss ratio of video decreases as the number of contention slots increases. The reason is as follows. In the static allocation scheme, as the number of contention slots increases, the uplink capacity for data transfer decreases and then becomes insufficient. That is, there exists a tradeoff between the bandwidth request efficiency and the capacity for the uplink bursts. Therefore, the optimal number of contention slots, which minimizes the MU loss ratio, exists. Even in this situation, the adaptive allocation scheme can use OFDM symbols which are not used in the downlink burst duration and then enhances the QoS compared to the static allocation scheme.

We also notice in Fig. 5 that for the static allocation scheme with the piggyback request mechanism, the number of contention slots which minimizes the MU loss ratio is smaller than that without the piggyback request mechanism. This is because the piggyback request mechanism can improve the efficiency of the bandwidth request, and then the number of received requests at BS increases.

We see in Fig. 5 that when the number of contention slots is equal to or larger than nine, the effect of piggyback request mechanism on the MU loss ratio of video is small. This is because the bandwidth for the uplink data transmission decreases as the number of contention slots increases in the static allocation scheme. Thus, it is difficult to be allocated the bandwidth as requested.

Furthermore, in Fig. 6, we notice that the static allocation scheme with the piggyback request has larger error concealment ratio than that without the piggyback request when the number of contention slots is larger than eight. This is because the bandwidth is granted partially under the condition.

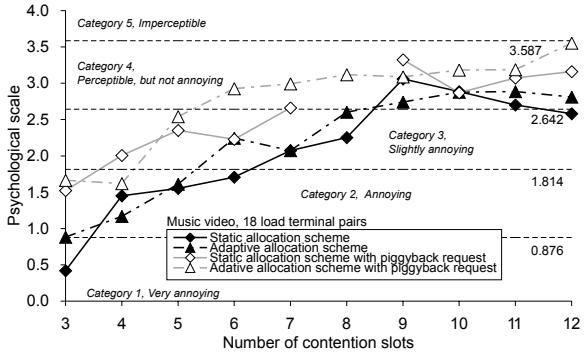

Fig. 7. Psychological scale values for music video with 18 load terminal pairs.

C. QoE

We calculated the interval scale from the obtained result of the rating–scale method. As a result of the Mosteller's test, we found that the null hypothesis that the obtained interval scale fits the observed data can be rejected at significance level 0.01. By removing seven stimuli which give large errors of Mosteller's test, we saw that the hypothesis cannot be rejected.

Note that we can select an arbitrary origin in an interval scale. In this paper, the origin is set to the minimum value of the psychological scale in the assessment. Under this condition, we also calculated the lower boundaries of the categories and got 3.587 for Category 5, 2.642 for Category 4, 1.814 for Category 3, and 0.876 for Category 2. The lower bound of category 1 is $-\infty$, and the upper bound of category 5 is ∞.

Figures 7 through 10 show the psychological scale values versus the number of contention slots. Figure 7 depicts the psychological scale value for music video with 18 load terminal pairs. This figure plots the results for four schemes obtained from the combination of the bandwidth request mechanisms and the capacity allocation schemes. Figure 8 shows the psychological scale value for sport in the same way as Fig. 7. The psychological scale values for music video and sport with 20 load terminal pairs are shown in Figs. 9 and 10, respectively.

In Figs. 7 through 10, we notice that for all the number of load terminal pairs and the capacity allocation schemes, the psychological scale values with the piggyback request mechanism are higher than those without the mechanism. In

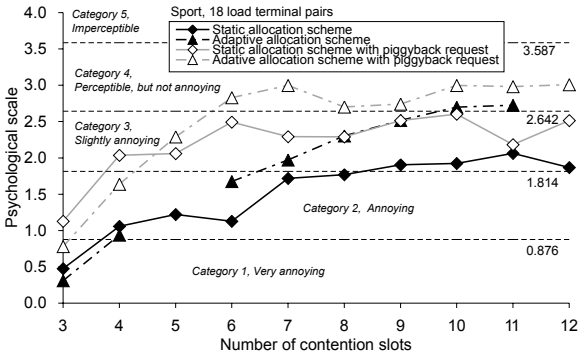

Fig. 8. Psychological scale values for sport with 18 load terminal pairs.

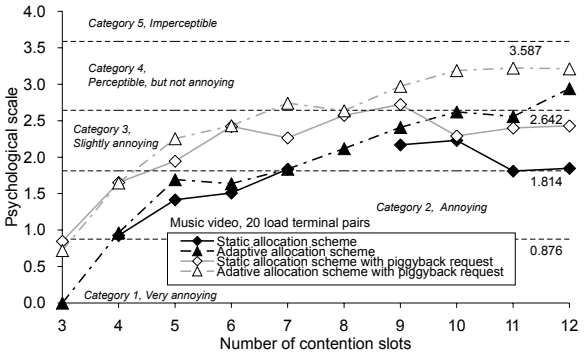

Fig. 9. Psychological scale values for music video with 20 load terminal pairs.

particular, the piggyback request mechanism is effective for sport with the number of contention slots from five to seven when the number of load terminal pairs is 18. Thus, the piggyback request mechanism can enhance QoE of the audio–video stream.

We also find in Figs. 7 through 10 that the adaptive allocation scheme can achieve higher QoE than the static allocation scheme when the number of contention slots is equal to or larger than five. This is because the adaptive allocation scheme can efficiently use OFDM symbols and then enhance the QoE.

On the other hand, we see in Figs. 7 through 10 that the psychological scale value with the adaptive allocation scheme is equal to or slightly smaller than that with the static allocation one when the number of contention slots is three or four. This is because the adaptive allocation scheme cannot efficiently use OFDM symbols owing to the small number of acceptable bandwidth requests under the condition.

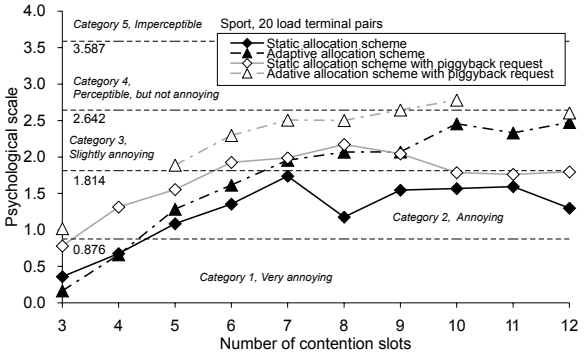

Fig. 10. Psychological scale values for sport with 20 load terminal pairs.

We see in Figs. 7 through 10 that the psychological scale values for music video tend to be larger than those for sport. This is because sport is a video–dominant content. In the assessment, the receiver conceals and outputs a video frame even if a piece of the frame is lost. The degradation of spatial quality due to the error concealment affects the QoE for sport more largely than that for music video.

In addition, we notice that the difference in the psychological scale values between the adaptive allocation scheme and the static allocation one for sport is larger than that for music video. It is also the effect of the difference of the contents.

VI. Conclusions

In this paper, we assessed the joint effects of the capacity allocation schemes and the piggyback bandwidth request mechanism on QoE of uplink audio–video transmission in the IEEE 802.16 network with the BE service. We employed two contents and two capacity allocation schemes: static allocation and adaptive allocation. As a result, we found that the piggyback bandwidth request is effective for QoE enhancement in both allocation schemes. In addition, the adaptive allocation scheme achieves higher QoE than the static allocation scheme. Furthermore, the effectiveness of the piggyback request and capacity allocation differs with the content.

As for future work, we need to assess QoE in various situations, i.e., various contents and network conditions.

Acknowledgments

The authors thank Yukihiro Nakao for his support in the simulation.

References

[1] ITU-T Rec. P.10/G.100, Amendment 2, "New definitions for inclusion in Recommendation ITU–T P.10/G.100," July 2008.
[2] Ustream.tv: You're On, (http://www.ustream.tv).
[3] IEEE Std. 802.16–2004, "Local and metropolitan area networks, part 16: air interface for fixed broadband wireless access systems", Oct. 2004.
[4] WiMAX Forum, "The WiMAX Forum Certified^{TM} program for Fixed WiMAX^{TM}", Jan. 2007.
[5] C. –H. Chiang, W. Liao and T. Liu, "Adaptive downlink/uplink bandwidth allocation in IEEE 802.16 (WiMAX) wireless networks: A cross–layer approach," *Conf. Rec. IEEE GLOBECOM 2007*, Nov. 2007.
[6] R. Pries, D. Staehle and D. Marsico, "IEEE 802.16 capacity enhancement using an adaptive TDD split," *Proc. IEEE VTC Spring '08*, May. 2008.
[7] D. Migliorini, E. Mingozzi and C. Vallati, "QoE–oriented performance evaluation of video streaming over WiMAX," *Wired/Wireless Internet Communications*, LNCS 6074, pp. 240–251, 2010.
[8] D. –B. Lee and H. Song, "QoE–aware mobile IPTV channel control algorithm over WiMAX network," *J. Vis. Commun. Image R.*, vol. 21, no. 3, pp. 245-255, Apr. 2010.
[9] The network simulator – ns–2 –, (http://www.isi.edu/nsnam/ns/).
[10] Seamless and Secure Mobility tool suite, (http://www.antd.nist.gov/seamlessandsecure/toolsuite.html).
[11] Design and Implementation of a QoS-included WiMAX Module for NS-2 Simulator, (http://perso.telecom-bretagne.eu/aymenbelghith/tools/).
[12] Aperto Networks :: PacketMAX Family, (http://www.apertonet.com/products/pmax.html)
[13] RedMAX^{TM} AN–100U Base Station, (http://www.redlinecommunications.com/en/products/redmax-wimax-family/an-100u-base-station)
[14] Y. Ito and S. Tasaka, "Tradeoff relationship between fidelity and latency in interactive audio–video applications over IP networks," *IEICE Trans. Commun.*, vol. E90–B, no. 5, pp. 1112–1121, May 2007.
[15] S. Tasaka, H. Yoshimi, A. Hirashima and T. Nunome, "The effectiveness of a QoE–based video output scheme for audio–video IP transmission," *Proc. ACM Multimedia2008*, pp.259–268, Oct. 2008.
[16] S. Tasaka and Y. Ito, "Psychometric analysis of the mutually compensatory property of multimedia QoS," *Conf. Rec. IEEE ICC 2003*, May. 2003.
[17] F. Mosteller, "Remarks on the method of paired comparisons: III a test of significance for paired comparisons when equal standard deviations and equal correlations are assumed," *Psychometrika*, vol. 16, no. 2, pp. 207–218, June 1951.